

Novel Possibilities for Coherent Radiation Sources

Yasser A. Hussein and James E. Spencer

Stanford Linear Accelerator Center, Stanford University, Menlo Park, CA, USA

Abstract — Higher frequency radiation sources and their detectors have many potential uses -- especially if they are compact, variable, efficient and have high brightness. We discuss some possibilities together with various impediments to their realization. The differences between bound and free electrons are studied from the standpoint of the frequencies that are practicably achievable. With the ansatz that the transport physics with Maxwell's Equations are valid but modified by the material properties, a number of analogs exist between these two basic sources of radiation. In many cases, the differences are between macro and micro implementations e.g. between klystrons and klystrinos (micro or nano) or solid state and semiconductor lasers or rare-earth doped transistors. Cases with no apparent analogs are ones due to unique quantum effects e.g. radiation at $3kT_c$ in superconductors. This is well above magnetic resonance imaging MRI around $0.4 \mu\text{eV}$ but well below room temperature at 25 meV . Bound and free possibilities for planar, micro undulators over this range are studied using FDTD techniques. To our knowledge, there have been no implementations of either possibility.

Index Terms — FDTD, (sub) millimeter radiation, micro undulators/wigglers, microwave photonics, THz technologies.

I. INTRODUCTION

Despite the considerable success in accessing the entire electromagnetic spectrum there are serious gaps e.g. on either side of what can be called the intrinsic laser band running from 100 nm or so up to $10 \mu\text{m}$ (30 THz) [1]. Because there appear to be advantages available for both pure and applied fields in other wavelength regions, these provide interesting research opportunities. While our discussion is not restricted to any particular frequency, we emphasize longer wavelengths [2,3] but shorter than typical masers.

While it is impossible to give a fair introduction and motivation for this subject, a good discussion on sensors, sources and their application drivers has been given [2] recently for the terahertz region. Two interesting aspects are the technical challenges and that most of the photons emitted since the Big Bang fall in this region from the far infrared FIR through the sub-millimeter range down to the limit of WR-3 waveguide at $\leq 300 \text{ GHz}$. Thus, such photons present another kind of cold, dark energy. We will assume that accurate modeling of active devices

necessarily involves solving the equations that describe production and transport based on Maxwell's Equations regardless of whether the electrons are free or bound.

II. GENERAL DISCUSSION

An important aspect of any source is the ability to measure it so we have placed a high value on reciprocity. Fast switching transistors or the production of x-rays via electron bremsstrahlung are classic examples of the inverse of the photoelectric effect that is used to produce electrons when the photon energy $h\nu$ has an energy sufficient to assist the electron in overcoming the Schottky barrier. The phase space densities of the resulting electron or photon beams depend on their wave vectors and both beams will diverge/diffract without confining potentials or guide structures that are properly matched to the incident beams. These are the reasons for the increased use of laser driven, RF assisted electron guns and photonic band gap crystals.

If one runs the resulting beam of free electrons into a macroscopic undulator [1] having a wavelength λ_U they will radiate at harmonics n of the device period:

$$\lambda \sim \frac{\lambda_U}{2n\gamma^2} \quad (1)$$

where the electron energy γ is in units of rest mass mc^2 . Clearly, one can benefit from increasing the energy or reducing λ_U or the effective mass m^* (making γ a tensor makes m an invariant). For low energy conduction band electrons, $\gamma \sim 1$ so that a wiggle period of $\lambda_U = 60 \mu\text{m}$, achievable with standard IC techniques, might be expected to give $30 \mu\text{m}$, 10 THz radiation. We explore the validity of these ideas and ways to implement such devices.

III. FDTD CODE VALIDATION

Finite Difference Time Domain (FDTD) is a powerful and flexible technique that is expected to play a central role in development and simulation of sub-millimeter wave devices. It was chosen over others because it is very efficient and its implementation is straightforward. Also, the FDTD method is ideal for our problem which is non-linear and may be anisotropic with single pulse currents.

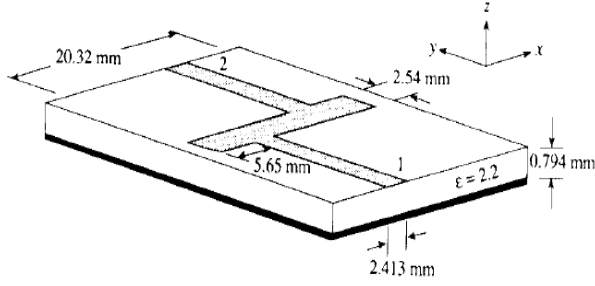


Fig. 1. Bench-mark filter used to validate the FDTD code.

Before presenting simulation results for any undulators, the developed FDTD code should be validated. The results are compared to those presented in [4]. The low-pass filter used to validate the code is shown in Fig. 1. Comparison results for the insertion loss (S_{21}) and return loss (S_{11}) are shown in Figs. 2 and 3. One observes good agreement with measured and calculated data except for the highest frequency which is somewhat shifted. Experimentation with planar circuit techniques leads one to conclude that this shift is caused mainly by the slight misplacement of the ports inherent in the choice of the spatial steps [4].

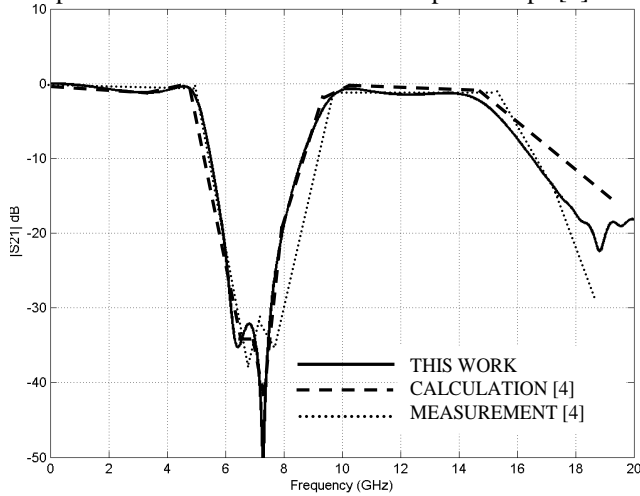


Fig. 2. Insertion loss comparison curves of the low-pass filter.

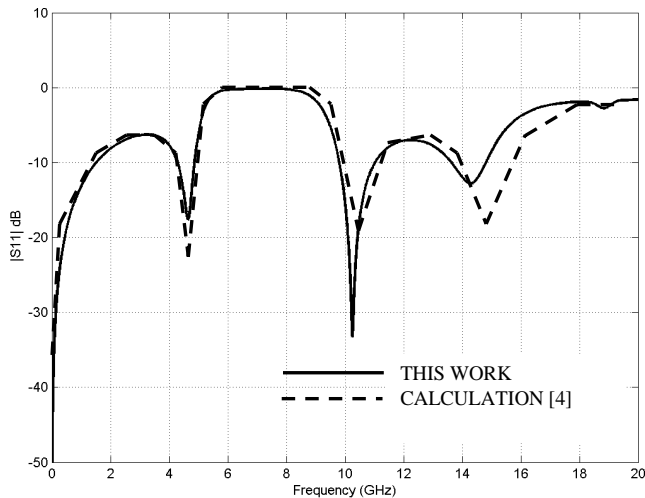


Fig. 3. Return loss comparison curves of the low-pass filter.

IV. ILLUSTRATIVE EXAMPLES

Figure 4 shows a sample, planar lattice for 1.5 periods of a two-dimensional (2-D) wiggler. Several examples of these structures have been printed with different periods and wavelengths [5] where dimensions were scaled to give the same low frequency impedances for similar periods. Pulse currents greater than 1 A at 1 ns were obtained routinely without failures by careful conditioning.

Different 2-D and 3-D implementations are interesting to pursue as well as other inductor-like topologies or laser driven, high mobility, direct band gap materials but first, it is useful to check the consistency between the classical and microscopic pictures we have assumed.

For conventional synchrotron radiation [6], one can estimate an energy loss per wiggler turn of:

$$U(\text{meV}) = \frac{3.0\gamma^4}{\rho(\mu)} \quad (2)$$

where $\rho(\mu)$ is the bend radius in μm . We note that Eq. (2) can be due to magnetic or other equivalent effects because any change in velocity or momentum of an electric charge results in radiation. Further, the average photon energy u can be written:

$$\langle u(\text{meV}) \rangle = \frac{94.3 \gamma^3}{\rho(\mu)} = 9.5 \quad (3)$$

where we have assumed a radius of $10 \mu\text{m}$ from Fig. (4). For reference, a 0.5 THz photon has an energy of $\sim 5 \text{ meV}$. Thus, the assumption of constant ρ in Eqs. (2)-(3) appears reasonable, ignoring intrinsic scattering in the material.

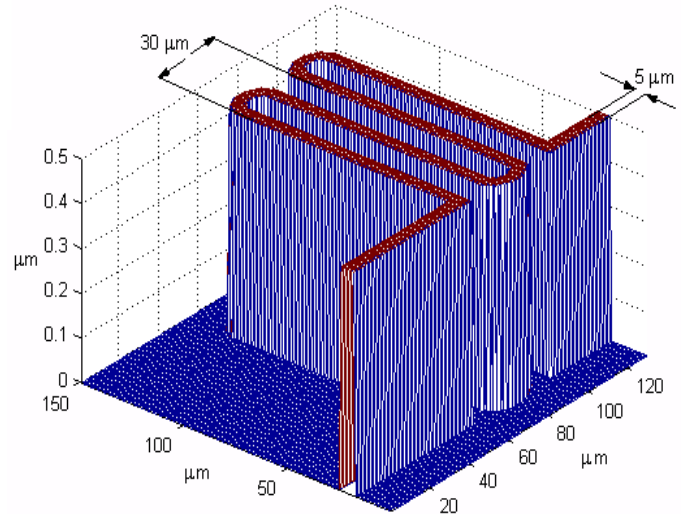


Fig. 4. Planar lattice (not to scale) for 1.5 periods of a 2-D wiggler with the vertical representing a perfect conductor of $0.5 \mu\text{m}$ thickness and “0” a dielectric substrate (Duriod: relative permittivity of 2.2).

V. SOME RESULTS AND DISCUSSION

FDTD simulations were carried out for wiggler structures such as shown in Fig. 4 for 1.5 periods. The half-period circuit length L is $231.4 \mu\text{m}$ for $\lambda_U = 30 \mu\text{m}$. This gives a fundamental resonant frequency f_0 of 0.437 THz . This is not f_U for a free electron from Eq. (1). The return loss for a half period and 1.5 periods are shown in Figs. 5 and 6 normalized to the frequency f_0 . None of these structures, in this form, are expected to be coherent.

Figure 5 demonstrates that an electron wave passes through the structure with very small reflection at f_0 because it doesn't resolve the half loop well at this frequency and so passes through it with virtually no reflection. Further, the broad reflections around $2, 4, 6,$ and $8 f_0$ are due to harmonics of the reflection coming from the loop at $1/4$ of the wiggler period. As the frequency increases, the reflection coefficient increases and broadens consistent with the fact that higher frequencies resolve and sample the full loop better. From Fig. 4, Eqs. (2)-(3) and f_0 we expect a radiation rate of ~ 0.03 photons per electron per half loop with a diffuse pattern based on a mean angular spread of $\sim 1/\gamma$ radians. While not optimal for brightness, it does imply out-of-plane radiation. We also expect the reflected electrons to radiate photons with a different radiation pattern in a competitive way because $\gamma \sim 1$.

In Fig. 6, there is now added reflection and transmission around f_0 corresponding to the same mechanism as in Fig. 5 for the strong single loop transmission at frequency f_0 . For coherence with such structures we would require multi-port feeds. In such cases, one could expect the three modulations to merge near f_0 with a more pronounced resonance structure. Another observation is that the broad reflections around $2, 4, 6,$ and $8 f_0$ exist also for the 1.5 period case except that the loops at $1/4, 3/4$ etc. of the period cause modulation in between. This explains why the reflections for the 1.5 period case trend higher than the half period case by direct analogy with HR coatings.

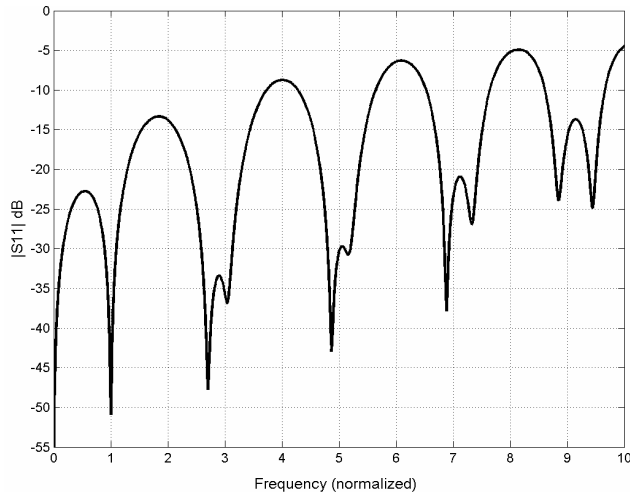


Fig. 5. Return loss versus f/f_0 for the 0.5 period wiggler.

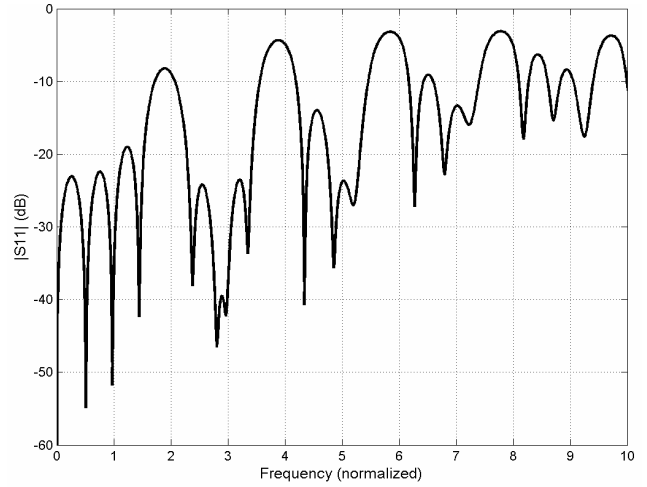


Fig. 6. Return loss versus f/f_0 for the 1.5 period wiggler.

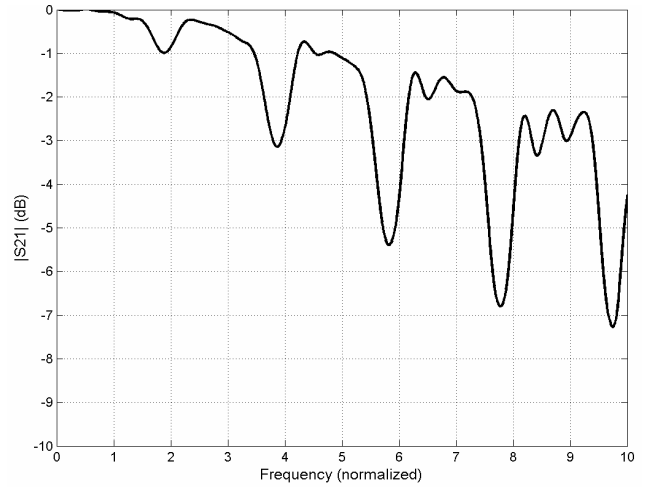


Fig. 7. Insertion loss versus f/f_0 for the 1.5 period wiggler.

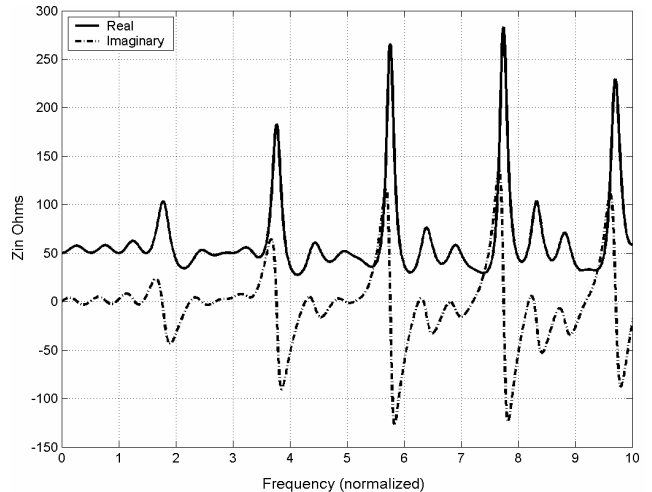


Fig. 8. Input impedance versus f/f_0 for the 1.5 period wiggler.

Figure 7 shows the insertion loss versus frequency for 1.5 periods. As the frequency increases, transmission decreases. This is dual to the return loss parameter.

Figure 8 shows the input impedance (real and imaginary) as a function of frequency. At deep resonance, the input impedances are purely real (50Ω). This corresponds to a matching load that has zero reflection. Under the assumption of ballistic transport, this implies a broad band radiation spectrum having the mean energy given by Eq. (3) although such radiative losses are not explicitly reflected in these plots.

On the other hand, the broad reflections around $2, 4, 6,$ and $8 f_0$ have higher values of input impedance (mismatching) emphasizing that many more electrons are reflected at these frequencies producing radiation with a more bremsstrahlung-like spectrum. This mode relates most closely to IMPATT devices. In both cases, ballistic transport and reflection, the spectra and distribution patterns are expected to be very different with the latter extending to higher frequencies and in lowest order having a dipole distribution whose axis is centered on the incident electron's wave vector so the radiation peaks in directions around the perpendicular to this vector. This is in direct contrast to the synchrotron-like radiation. With increasing frequencies we expect such differences to become better defined because the classical conditions for radiation [6] improve. Clearly, we need to compute the far field distributions at discrete frequencies to verify this. Work is being done now to obtain the radiation fields using the Ansoft high-frequency structure simulator HFSS.

To obtain a bound, micro undulator that retains the 2-D structure of Fig. 4, we can add a thin covering dielectric layer followed by a broad strip of metal running perpendicular to the straight segments as shown in Fig. 9. This is pulsed with shorter duration, higher peak currents that couple to the fields of the previous circuit to produce coherent radiation (Eq. 1) whose wavelength varies with the angle of observation relative to the oscillation plane. This relates to Smith Purcell radiation [7] but is more practical. There are many variants. For the free case one can add a mirror symmetric circuit above Fig. 4.

A useful figure-of-merit for such devices is the 6-D, normalized brightness in the form of a photon density:

$$B_n^6 = (4\pi)^2 \frac{N_\gamma}{\lambda^2 \sigma_i \sigma_\omega / \bar{\omega}} \eta \leq 7 \cdot 10^{16} \eta / \lambda^3. \quad (4)$$

Even for $\eta \ll 1$, bound implementations are far preferable since this is an intense source by virtually any standard.

Even the differing uses of metals in such devices, as opposed to semiconductors, is too broad to discuss here as well as the differences between metals such as Al and Au for use in fast laser drive systems [8] but we would be remiss to not mention materials such as poled, periodic lithium niobate [9] that could also be used with electrons.

CONCLUSIONS

We have argued that bound implementations have many advantages but cost savings, based on using the same standard IC techniques used for compactness, could be remarkable compared to macro FELs operating at tens of MeV with their operational and other disadvantages. We are now calculating angular and energy distributions.

ACKNOWLEDGEMENT

This work was supported by the US Department of Energy under contract *DE-ACO3-76SF00515*.

REFERENCES

- [1] Free electron lasers (FELs) based on undulators extend this region as does nonlinear HG with lasers but with reduced intensities. *Synchrotron Radiation Research*, H. Winick and S. Doniach, Ed's. New York: Plenum Press 1980.
- [2] Peter H. Siegel, "Terahertz Technology", *IEEE Trans. Microwave Theory Tech.*, vol. 50, No. 3, Mar. 2002.
- [3] S. James Allen, "Terahertz Dynamics in Semiconductor Quantum Structures", *27th Int'l. Conf. IR and Millimeter Waves*, Sept. 2002.
- [4] D. M. Sheen, *et al.*, "Application of the three-dimensional finite-difference time-domain method to the analysis of planar microstrip circuits," *IEEE Trans. Microwave Theory Tech.*, vol. 38, pp.849-857, July 1990.
- [5] Wanil Ha, *et al.*, "Miniaturization Techniques for Accelerators", *2003 Part. Accel. Conf.*, May 2003.
- [6] Julian Schwinger, "On the Classical Radiation of Accelerated Electrons", *Phys. Rev.*, June 1949.
- [7] S.J. Smith and E.M. Purcell, "Visible Light from Localized Surface Charges Moving across a Grating", *Phys. Rev.* 92, Aug. 1953.
- [8] C. Guo *et al.*, "Structural Phase Transition of Aluminum Induced by Electronic Excitation", *Phys. Rev. Lett* 84, May 2000.
- [9] C. Weiss *et al.*, "Generation of tunable narrowband surface-emitted THz-radiation in periodically poled Lithium Niobate", *Opt. Lett.* 26, 2001.

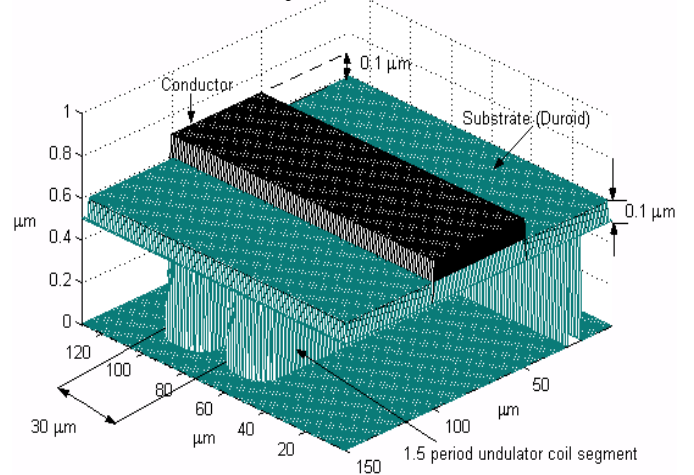


Fig. 9. 1.5 period segment of a 2-D undulator based on Fig. 4.